https://doi.org/10.32604/zkg.2024.03.01

Research on the correlation between autogenous shrinkage and compressive strength of mortar modified by styrene-butadiene rubber

Junpeng Mei[1, 2, 3], Jiacheng Xie[1], Yanjun Zhao[4], Yinlong Niu[4], Zhixin Wang[1] and Shuang Li[1]
[1]School of Urban Construction, Wuhan University of Science and Technology, Wuhan 430065/China
[2]Hubei Provincial Engineering Research Center of Urban Regeneration, Wuhan 430065/China
[3]Institute of High Performance Engineering Structure, Wuhan University of Science and Technology, Wuhan 430065/China
[4]China Construction Third Bureau First Engineering Co., Ltd., Wuhan 430040/China

ABSTRACT: In this paper, the effects of styrene-butadiene rubber (SBR, 1%~4%) powder on the autogenous shrinkage and compressive strength of cement-based materials at 3, 7, 28, 60 and 90 d were firstly studied, then the mechanism behind was investigated by means of X-ray diffraction (XRD), Fourier transform infrared spectroscopy (FTIR), scanning electron microscope (SEM) and mercury intrusion porosimetry (MIP), and at last the correlation between autogenous shrinkage and compressive strength was analyzed by establishing a mathematic model. Results show that the appropriate dosage of SBR reduces the dissolution rate of cement clinker, delays the arrival of the acceleration period, reduces the formation of hydration products, decreases the early hydration rate and inhibits the pozzolanic reaction between $Ca(OH)_2$ and fly ash, thus reducing the autogenous shrinking and compressive strength of cement-based materials. In addition, there is a good linear correlation between autogenous shrinkage and compressive strength of SBR modifi ed cement mortar, and such results can provide some reference for predicting autogenous shrinkage by compressive strength in practical engineering.

MATERIALS

1. Introduction

Autogenous shrinkage is the self-deformation of cement-based materials independent of ambient temperature and humidity changes and external load conditions, and is the sum of self-drying shrinkage and chemical shrinkage[1]. In recent years, the strength requirement of engineering concrete has been increasing, and the water-cement ratio are constantly decreasing, resulting in a large number of cracks caused by autogenous shrinkage, which seriously aff ects the service life of concrete. In view of the problem of large autogenous shrinkage of high performance civil engineering materials, many scholars have tried to use diff erent means to improve, such as cement modification[2], adding shrinkage reducer[3], expansion agent[4, 5], mineral admixture[6, 7], fi ber [8, 9] and so on. In addition, using polymer to reduce the autogenous shrinkage of cement-based materials is also a common method.

Styrene-butadiene rubber (SBR) powder is a commonly used polymer modifier, and the addition of SBR to cement-based materials can signifi -cantly improve the microstructure[10], increase the tensile and adhesive strength[11], and reduce the autogenous shrinkage of the samples[12, 13]. In engineering practice, autogenous shrinkage measurement is difficult and time-consuming, so the correlation model between autogenous shrinkage and compressive strength can be established to predict the autogenous shrinkage value.

Based on this, the infl uences of styrene-butadiene rubber (SBR, 1% ~ 4%) powder on the auto-genous shrinkage and compressive strength of cement-based materials at 3, 7, 28, 60 and 90 d were investigated, and the mechanism behind was studied by means of XRD, FTIR, SEM and MIP. Simultaneously, the correlation mathematical model between autogenous shrinkage and compressive strength was established according to the test data, which provides a certain reference for predicting the related properties of modified mortar in practical engineering.

2. Experiment

2.1 Raw materials

In the experiment, P·O 42.5 cement and Class F Grade II fly ash (FA) were used, and their chemical compositions are shown in Table 1, respectively. The fine aggregate is quartz sand with a particle size of 20 ~ 80 mesh. The water reducing agent is polycarboxylate superplasticizer (PCE) with solid content of about 50% (mass fraction). The polymer used for the modification of cement-based material was PSB150 styrene-butadiene rubber (SBR) powder with solid content ≥ 98% (mass fraction) and average particle size of 85 μm. The anti-foam

All authors

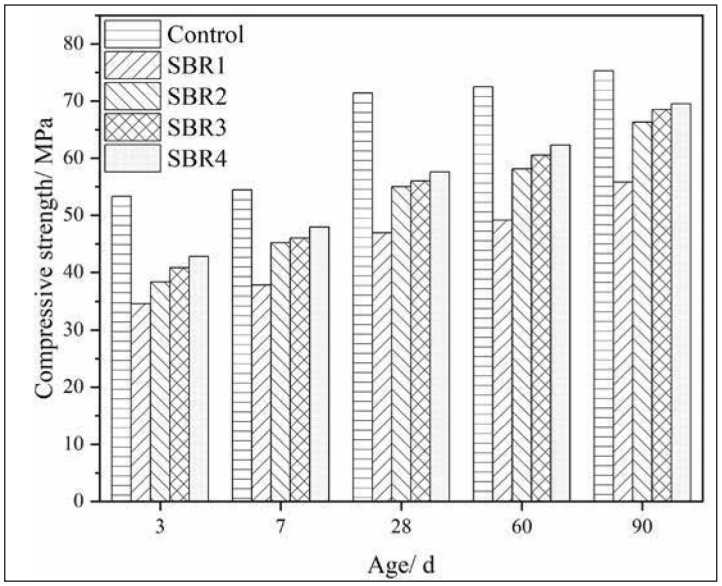

1 Influence of different SBR contents on the compressive strength of mortars

additive (AA) is a modified silicone defoamer, a transparent liquid with an effective composition of 98%. Wuhan tap water was used as mixing water.

2.2 Sample preparation

The mix proportions of cement-based materials are shown in Table 2. The binders are composed of cement and FA, and FA accounts for 20% of the mass of the binders. The water-binder ratio and the sand-binder ratio of the sample are 0.25 and 1.5, respectively. The content of SBR and PCE are 1% ~ 4% and 0.5% of the mass of the binders, respectively, and the content of AA is 3% of the mass of SBR.

The mix proportions of the pastes used for micro-measurement is the same as that of the mortars without sand, and the stirring is carried out according to GB/T1346-2011[14]. The samples cured to a certain age were broken into small pieces and the middle parts were selected to immerse in absolute ethyl alcohol to terminate hydration. Some of the small pieces are used for SEM and MIP tests, and the others are ground into powders for XRD and FTIR tests.

2.3 Test method

2.3.1 Compressive strength

The compressive strength tests of mortars were carried out according to GB/T 17671-1999[15], with the specimen size of 40 mm × 40 mm× 160 mm and the loading rate of 2.4 kN/s.

2.3.2 Autogenous shrinkage

In the autogenous shrinkage test, the specimens with the size of 25 mm × 25 mm × 280 mm were prepared according to JC/T 603-2004[16], and the standard length of the samples was measured after 24 hours of standard maintenance (> 90% R.H. and 20 ± 1 °C). After that, all specimens were sealed with aluminum foil tape, and the length of the specimens was measured after curing to a specific age, and the assessment of the autogenous shrinkage rate was conducted at different ages.

2.3.3 XRD

XRD tests were conducted by Bruker D8 Advance X-ray diffractometer with a scanning angle of 10° ~ 70° and a scanning rate of 8 (°)/min.

2.3.4 FTIR

FTIR tests were performed by a Nicolet iS50 infrared spectrometer with a wavenumber range of 4000 ~ 400 cm^{-1}.

2.3.5 SEM

JSM-6610 scanning electron microscope (SEM) with an acceleration voltage of 20 kV and the working distance of about 20 mm under vacuum environment was used to observe the surface morphology of cement paste samples.

2.3.6 MIP

PoreMaster-33 mercury intrusion porosimeter with a contact angle of 140° was used to characterize the pore structure.

3. Results and discussion

3.1 Compressive strength

Figure 1 shows the influence of different SBR contents on the compressive strength of mortars.

1 Main chemical composition of cement and fly ash

Material	Chemical composition (wt. %)								
	CaO	SiO_2	Al_2O_3	Fe_2O_3	MgO	Na_2O	K_2O	SO_3	LOI
Cement	60.08	19.73	5.97	3.54	1.77	0.11	0.93	2.77	4.21
FA	3.99	44.83	35.25	4.14	0.27	0.42	1.24	1.40	7.31

2 Mix proportions of the mortars

Code	Cement/g	FA/g	Sand/g	Water/g	SBR/%	AA/g	PCE/%
Control	576	144	1080	180	/	/	0.5%
SBR1	576	144	1080	180	1%	0.216	0.5%
SBR2	576	144	1080	180	2%	0.432	0.5%
SBR3	576	144	1080	180	3%	0.648	0.5%
SBR4	576	144	1080	180	4%	0.864	0.5%

It is obvious from Figure 1 that the compressive strength of cement mortar decreases with the addition of SBR, mainly because the adsorption and complexation of SBR hinder the early hydration of binders. However, the strength gradually increases with the rise of SBR content, although it is still lower than that of the control sample, mainly for the following reasons [17]: First, the polymer chain contains a large number of benzene rings, which occupy a larger volume after polymerization, which can better fill the pores, improve the microstructure compactness, and thus increase the compressive strength; Second, the addition of SBR promotes the formation of AFt and improves its stability in cement-based materials, which can also increase the compressive strength of the sample.

3.2 Autogenous shrinkage

It can be seen from Figure 2 that the autogenous shrinking rate of the sample can be reduced by adding a proper amount of SBR, while the shrinking rate can be greatly increased and the volume stability is decreased when the SBR content is large. Specifically, the autogenous shrinkage rate of mortars with 1% and 2% SBR at 3 d is 15.1% and 73.4% lower than that of the control sample, respectively, at 28 d is 0.9% and 1.6% lower, and at 90 d is 0.6% and 10.3% lower. While the autogenous shrinkage rate of the sample with 3% and 4% SBR at 28 d are 27.3% and 51.6% higher than that of control sample, and at 90 d is 8.5% and 30.8% higher.

The mechanism of reducing the autogenous shrinkage of cement mortar by the incorporation of a proper amount of SBR mainly includes three aspects[18-21]: First, SBR can be adsorbed on cement clinker, reducing the hydration rate and water consumption, and therefore maintaining high relative humidity and decreasing the capillary tension and autogenous shrinkage. Second, the film formation of SBR restricts the movement of water in the pores and between the C-S-H layers, which is conducive to maintaining a high relative humidity in the pores and reducing the volume shrinkage deformation of C-S-H, and thus the autogenous shrinkage of the system is decreased. Third, SBR is interleaved with hydration products to act as a "microfiber" and offset some of the shrinkage stress, and therefore reduce the autogenous shrinkage of mortar. However, when the amount of SBR is too large, the air entraining effect would cause a large amount of shrinkage[22].

4. Mechanism analysis and model

4.1 Mechanism analysis

4.1.1 Hydration products

It can be seen from Figure 1 and Figure 2 that with the extension of age, the hydration reaction of cement continues, and the autogenous shrinking and compressive strength of modified mortar increase. On the one hand, in the cement hydration process, the consumption of water and the formation of hydration products would lead to the decrease of relative humidity in pores, the sharp increase of capillary tension and the rise of autogenous shrinkage. On the other hand, the hydration of cement generates a large number of C-S-H gels, and the ionic and covalent bonds between the C-S-H layers work together, and simultaneously, there are van der Waals forces between the particles, resulting in the formation of silicate polycondensation with a certain rigid structure, which makes the hardened cement paste have a high strength.

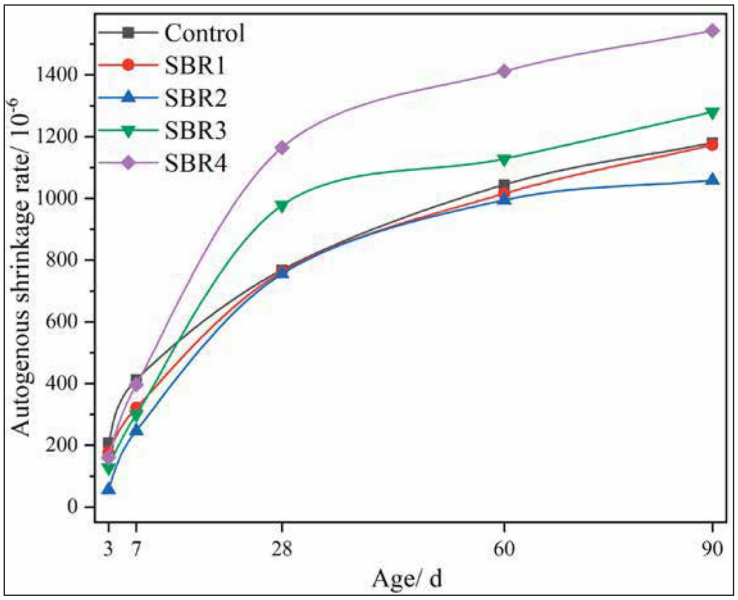

2 Autogenous shrinkage rate of mortars with different SBR contents and ages

From the above discussion, it can be seen that the changes of autogenous shrinking and compressive strength are inseparable from the hydration reaction, and there must be a correlation between them. Actually, the hydration reaction process of cement can be simply summarized as the dissolution of each mineral phase in cement and the precipitation of hydration products[19]. The hydration process mainly includes the dissolution of calcium silicate and the precipitation of C-S-H and CH, and therefore, the determination of undissolved calcium silicate (CS) content and CH content in cement paste can indirectly reflect the hydration degree of cement.

Figure 3 shows the XRD patterns of control and SBR2 samples at 3 and 28 d, and the hydration degree of cement is indirectly compared by comparing the strongest peak value of unhydrated CS and CH in the XRD patterns.

As shown in Figure 3, no new diffraction peak is found in the XRD pattern, indicating that the type of hydration products of the sample is not changed by addition of SBR. However, at 3 d, the diffraction peak intensity of C_3S and C_2S of the sample with SBR is stronger that of the control

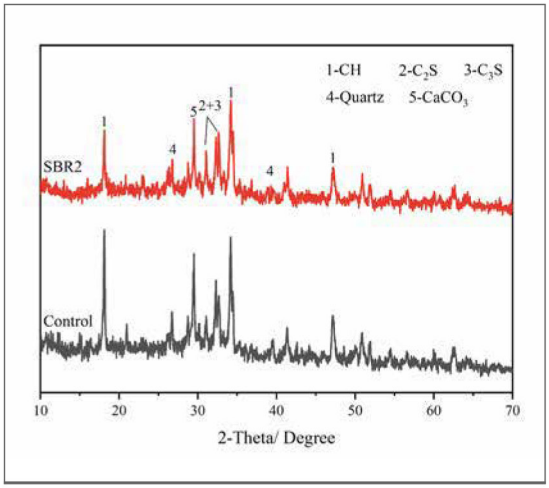

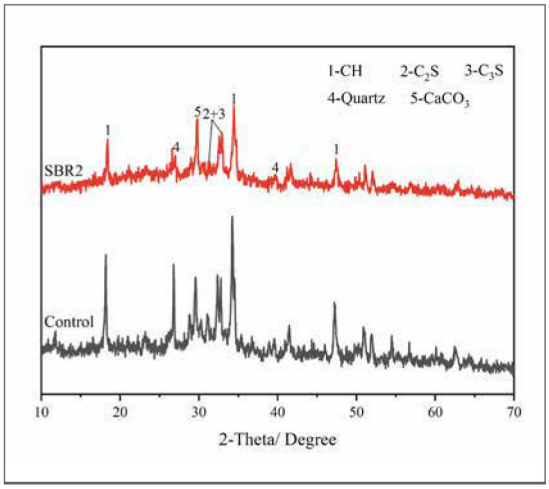

3 XRD patterns of Control and SBR2 samples at 3 and 28 d (a) 3 d (b) 28 d

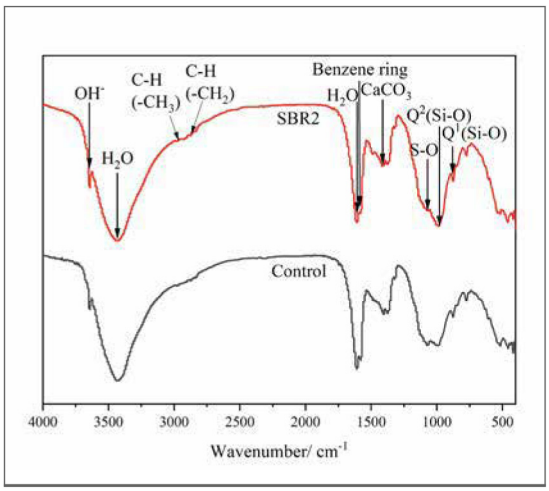

4 FTIR spectra of different samples at 28 d

sample, which is because SBR can be adsorbed on the surface of cement clinker, preventing its dissolution and reducing the hydration reaction rate. At 28 d, the diffraction peaks of C_3S and C_2S have the same peak variation law, that is, after the incorporation of SBR, there is more undissolved calcium silicate in the sample no matter at 3 d or 28 d, showing the low cement hydration degree.

In addition, the CH diffraction peaks of SBR2 are also lower than that of the control sample, mainly because at early age, SBR can reduce the hydration reaction rate, at the same time, complex free calcium ions in the solution, reduce the concentration of calcium ions, delay the supersaturation of CH and the arrival of the hydration acceleration period [23, 24], and thus reduce the content of CH; At late age, although the inhibitory effect of SBR on the activity of fly ash can reduce the consumption of CH, the obstacle to the formation of CH is more obvious, so the amount of CH is still reduced.

In order to further elucidate the effect of SBR incorporation on hydration products at 28 d, the FTIR tests were performed and the results are shown in Figure 4.

As shown in Figure 4, vibration peaks related to C-H bonds in $-CH_3$ and $-CH_2$ appear in the vicinity of 2960 cm^{-1} and 2870 cm^{-1} in the SBR2 sample, respectively, and a vibration peak related to benzene rings appears in the vicinity of 1600 cm^{-1}. In control sample and SBR sample, both Q^1 and Q2 vibration peaks are found near 876 cm^{-1} and 986 cm^{-1}, which are caused by Si-O bond stretching vibration. Compared with the Control sample, the Q^1 vibration peak of the SBR sample is slightly decreased, and the Q^2 vibration peak spectrum band is wider, indicating that the addition of SBR makes the amount of C-S-H generation and the polymerization degree reduced, and shortens the tetrahedral chain [25].

The changes of hydration degree of cement and the generation amount and polymerization degree of C-S-H gels can explain the change law of compressive strength and self-shrinkage of the samples to a certain extent. From the above discussion, it is evident that the incorporation of 2% SBR reduces the cement hydration degree and the generation amount and polymerization degree of C-S-H gels, so the compressive strength is reduced, and the reduction of hydration degree leads to the decrease of free water consumption, so the autogenous shrinkage is also reduced.

4.1.2 SEM analysis

In order to further explore the influence of SBR on the microstructure of samples, SEM tests were conducted on control and SBR2 samples at 3 d and 28 d respectively, and the results are shown in Figure 5.

As can be seen from Figure 5, at 3 d, many fibrous and granular hydration products are present in the control sample, the overall structure is loose and there are a lot of pores between the hydration products and cement clinker. In addition, many hydration products appear on the fly ash microspheres on the surface of the control sample, indicating that the pozzolanic reaction of the fly ash has begun. The hydration products in SBR2 sample are mostly in intermediate

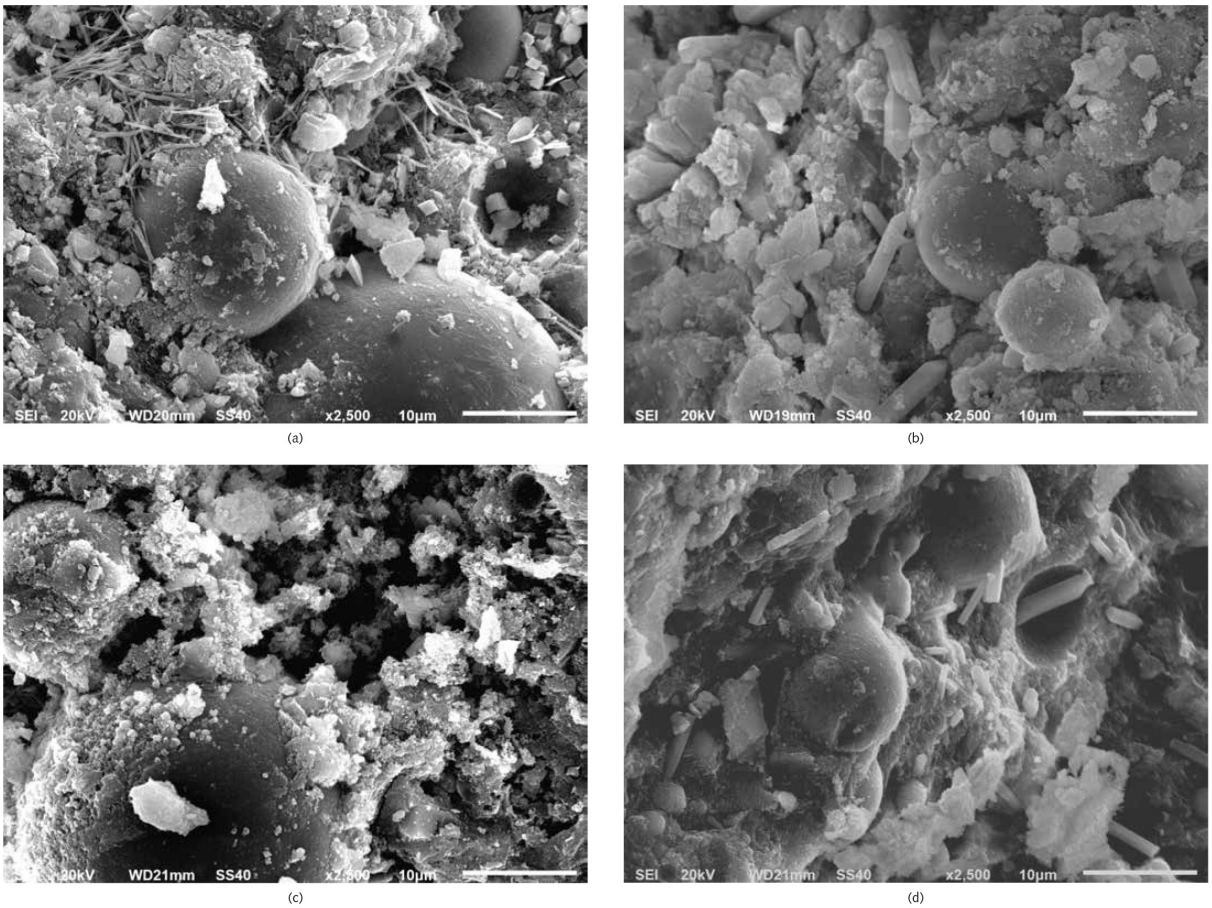

5 SEM images of control and SBR2 samples at 3 d and 28 d
(a) Control 3 d
(b) SBR2 3 d
(c) Control 28 d
(d) SBR2 28 d

form such as clusters and particles, and there are few lamellar gels, poor bonding between gels, and many holes and cracks. Moreover, the surface of fly ash microspheres is smooth, and no obvious hydration products are generated, so the compressive strength of the sample decreases. At 28 d, the overall hydration degree of the samples is higher than that at 3 d. Moreover, there are a large number of layered hydration products on the surface of fly ash microspheres in the control sample, which indicates that the pozzolanic effect of fly ash is very obvious, but the surface of fly ash microspheres in the SBR2 sample is smooth, showing that the reaction degree of fly ash is lower than that in the control sample. All these prove that SBR can inhibit the pozzolanic reaction of fly ash.

4.1.3 Pore structure analysis

The pore structure distribution of different samples at 28 d is shown in Figure 6, and pore structure parameters are shown in Table 3.

The pore size of cement-based materials can be divided into harmless pores (< 20 nm), less harmful pores (20 ~ 50 nm), harmful pores (50 ~ 200 nm) and very harmful pores (> 200 nm), among which the harmful pores and very harmful pores larger than 50 nm have a greater impact on the strength of cement-based materials[26]. Compared with the control sample, the harmful pores and very

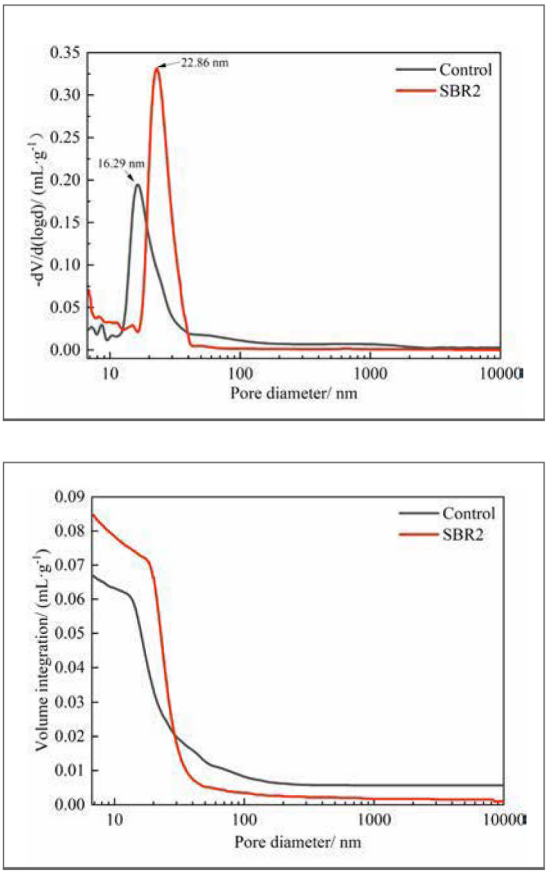

6 Pore structure distribution of different samples at 28 d (a) Differential curve (b) Integral curve

3 Pore size distribution of different samples

Sample	Total pore	Pore-size distribution (ml.g^{-1})			
	volume (ml.g^{-1})	<20 nm	20~50 nm	50~200 nm	>20 nm
Control	0.0670	0.0338	0.0211	0.0063	0.0058
SBR2	0.0857	0.0204	0.0601	0.0027	0.0025

harmful pores in the SBR2 sample which have a greater influence on the strength are reduced from 0.0121 ml·g^{-1} to 0.0052 ml·g^{-1}, which indicates that the addition of SBR can promote the transformation of harmful pores and very harmful pores to less harmful pores, and is conducive to improving the strength of the sample. While in fact, the incorporation of SBR results in a decrease in sample strength, which proves that the strength of cement-based materials is not only related to the pore structure, but also related to the type and quantity of hydration products. Although the addition of SBR improves the pore structure and size distribution of the sample, it also delays the hydration of cement-based materials and reduces the amount of hydration products, so the strength is decreased when the SBR is added.

It is well known that the shrinkage of cement-based materials is caused by the migration and consumption of internal pore water and the smaller the aperture, the greater the surface tension of the water. From Table 3, it is obvious that the addition of the 2% SBR decreases the pores smaller than 20 nm by 39.6%, and thus the autogenous shrinkage is reduced accordingly.

4.2 Correlation model between autogenous shrinking and compressive strength

In order to analyze the correlation between auto-genous shrinking (ε_{as}) and compressive strength (f_c), a regression equation including time (t), autogenous shrinking (ε_{as}) and compressive strength (f_c) was established. Compressive strength is the independent variable x= f_c (t), self-shrinkage is the dependent variable y=ε_{as} (t), and t is the time variable. The least square method was used for correlation analysis and in order to facilitate the establishment of the model, the input variables were transformed, i.e. X=x/ f_c (90), Y=y/ ε_{as} (90), and the relevant test data transformed are shown in Table 4. The linear fitting was performed on the test data, and the fitting results were shown in Table 5.

It can be seen from Table 5 that the correlation coefficient (R^2) can reach higher than 0.90, that is, there is a good linear correlation between compressive strength and self-shrinkage.

Based on the above regression analysis, the following mathematical model can be summarized:

$$Y = aX + b \quad (1)$$

Where a and b are constants of regression analysis.

5. Conclusion

1. The autogenous shrinkage of cement-based materials decreases with the appropriate amount of SBR (not more than 2%), while with the increase of SBR content (higher than 2%), the autogenous shrinkage increases again.
2. The addition of SBR makes the compressive strength of cement-based material lower than the control sample, but with the increase of SBR content, the compressive strength increases.
3. The main reason for the reduction of compressive strength and autogenous shrinkage by appropriate SBR is to delay the hydration process of cement and the secondary hydration process of fly ash. At 28 d, this retarding effect still exists, which is manifested by more unhydrated calcium silicate (CS) in the hardened paste and inhibiting the pozzolanic effect of fly ash.

4 Relative values of autogenous shrinking and compressive strength of different samples

Code	Control		SBR1		SBR2		SBR3		SBR4	
	X	Y	X	Y	X	Y	X	Y	X	Y
3 d	0.7078	0.1763	0.6201	0.1506	0.5777	0.0523	0.5956	0.0997	0.6158	0.1036
7 d	0.7224	0.3492	0.6774	0.2734	0.6817	0.2330	0.6715	0.2340	0.6892	0.2565
28 d	0.9482	0.6508	0.8405	0.6489	0.8296	0.7136	0.8175	0.7635	0.8288	0.7539
60 d	0.9628	0.8847	0.8799	0.8656	0.8763	0.9390	0.8832	0.8813	0.8964	0.9145
90 d	1.0000	1.0000	1.0000	1.0000	1.0000	1.0000	1.0000	1.0000	1.0000	1.0000

5 Fitting results of autogenous shrinking and compressive strength of different samples

Code	Fitting equation	R2
Control	Y = 2.3623X - 1.4389	0.9161
SBR1	Y = 2.3522X - 1.3025	0.9757
SBR2	Y = 2.4936X - 1.3900	0.9466
SBR3	Y = 2.4255X - 1.3291	0.9530
SBR4	Y = 2.5387X - 1.4406	0.9579

4. After the incorporation of SBR, there is a certain correlation between the compressive strength, autogenous shrinkage and hydration degree of the sample. A mathematical model of the correlation between compressive strength and autogenous shrinkage was established through regression analysis, that is, Y = aX + b. This model has certain reference value for predicting autogenous shrinkage in practical engineering.

6. Acknowledgement

"The 14th Five Year Plan" Hubei Provincial advantaged characteristic disciplines (groups) project of Wuhan University of Science and Technology (2023D0503) and the State Key Laboratory of Silicate Materials for Architectures (Wuhan University of Technology) (SYSJJ2022-20) are gratefully acknowledged.

REFERENCES

[1] Yang QB. Self-desiccation mechanisms of high-performance concrete [J]. Journal of the Chinese Ceramic Society, 2000, 28 (S1): 72-75
[2] Lefever G, Aggelis, DG, De Belie, N, et al. The influence of superabsorbent polymers and nanosilica on the hydration process and microstructure of cementitious mixtures [J]. Materials, 2020, 13 (22): 5194
[3] Hu S, Cai HB, Liu Q, et al. Development of a new type sprayed high ductility concrete (SHDC) and uniaxial compression test of rock-SHDC combined body [J]. Construction and Building Materials, 2023, 403: 132989
[4] Liu LM, Fang Z, Huang ZY, et al. Effects of expansive agent and super-absorbent polymer on performance of ultra-high performance concrete [J]. Journal of the Chinese Ceramic Society, 2020, 48 (11): 1706-1715
[5] Wang YJ, Tian Q, Li H, et al. Humidity sensitivity of hydration of expansive agent and its expansive efficiency in ultra-high performance concrete [J]. Crystals, 2022, 12 (2): 195
[6] Tertnkhajornkit P, Nawa T, Nakai M, et al. Effect of fly ash on autogenous shrinkage [J]. Cement and Concrete Research, 2005, 35 (3): 473-482
[7] Lee KM, Lee HK, Lee SH, et al. Autogenous shrinkage of concrete containing granulated blast-furnace slag [J]. Cement and Concrete Research, 2006, 36 (7): 1279-1285
[8] Guo AF, Sun ZH, Satyavolu J. Impact of modified kenaf fibers on shrinkage and cracking of cement pastes [J]. Construction and Building Materials, 2020, 264: 120230
[9] Shen DJ, Wen CY, Zhu PF, et al. Influence of Barchip fiber on early-age autogenous shrinkage of high-strength concrete internally cured with super absorbent polymers [J]. Construction and Building Materials, 2020, 264: 119983
[10] Heng YY, Zhao WJ. Research development of polymer modified cement based materials [J]. Bulletin of the Chinese Ceramic Society, 2014, 33 (2): 365-371
[11] Assaad JJ. Development and use of polymer-modified cement for adhesive and repair applications [J]. Construction and Building Materials, 2018, 163: 139-148
[12] Sadrmomtazi A, Khoshkbijari RK. Bonding durability of polymer-modified concrete repair overlays under freeze-thaw conditions [J]. Magazine of Concrete Research, 2017, 69 (24): 1268-1275
[13] Ramli M. Development of a durable polymer-modified cement matrix for ferrocement [D]. Sheffield: University of Sheffield, 1997
[14] GB/T14684-2011, Sand for construction [S]. Beijing: Standards Press of China, 2011
[15] GB/T 17671-1999, Method of testing cements–Determination of strength [S]. Beijing: Standards Press of China, 1999
[16] JC/T 603-2004, Standard test method for drying shrinkage of mortar [S]. Beijing: Standards Press of China, 2004
[17] Wang R, Wang PM. Effect of styrene-butadiene rubber latex/powder on cement hydrates [J]. Journal of the Chinese Ceramic Society, 2008, (7): 912-919+926
[18] Zhang GF, Wang PM. Effects of ethylene/vinyl chloride/vinyl laurate redispersible terpolymer on pore structure and properties of cement mortar [J]. Journal of Building Materials, 2013, 16 (1): 111-114+120
[19] Kong XM, Lu ZC, Zhang CY. Recent development on understanding cement hydration mechanism and effects of chemical admixtures on cement hydration [J]. Journal of the Chinese Ceramic Society, 2017, 45 (2): 274-281
[20] Lu Y, Wan XM, Guo SY, et al. Research on durability of epoxy resin modified alkali-activated slag based repair mortar [J]. Concrete, 2021, (1): 122-126
[21] Wang R, Xu YD. Influence of curing temperature on physical and mechanical properties of styrene-butadiene rubber latex/sulphoaluminate cement mortar [J]. Journal of the Chinese Ceramic Society, 2017, 45 (2): 227-234
[22] Jiang YQ. Application foundation of concrete admixture [M]. Beijing: Chemical Industry Press, 2013
[23] Kong XM, Emmerling S, Pakusch J, et al. Retardation effect of styrene-acrylate copolymer latexes on cement hydration [J]. Cement and Concrete Research, 2015, 75, 23-41
[24] Li HJ. Effect of Sulphoaluminate Cement and Styrene Butadiene Latex on Properties of Cement-based Patching Materials [J]. China Powder Science and Technology, 2016, 22 (1): 105-108
[25] Hughes TL, Methven CM, Jones TGJ, et al. Determining cement composition by Fourier transform infrared spectroscopy [J]. Advanced Cement Based Materials, 1995, 2 (3): 91-104
[26] Wu ZW. An approach to the recent trends of concrete science and technology [J]. Journal of the Chinese Ceramic Society, 1979, 7 (3): 262-270